

TOPMESH

A Tool for Extracting Topological Information from Non-manifold Objects

Leila De Floriani, Laura Papaleo

Department of Information and Computer Science, University of Genova, Italy

Annie Hui

Department of Computer Science, University of Maryland, U.S.A.

Keywords: Shape Modelling, Shape Understanding, Structural Representation, Non-manifold Geometry.

Abstract: We present *TopMesh*, a tool for extracting topological information from non-manifold three-dimensional objects with parts of non-uniform dimensions. The boundary of such objects is discretized as a mesh of triangles and of dangling edges, representing one-dimensional parts of the object. The geometrical and topological information extracted include the number of elements in the mesh, the number of non-manifold singularities and the *Betti numbers*, which characterize the topology of an object independently of the discretization of its boundary. *TopMesh* also computes a decomposition of the mesh into connected parts of uniform dimension, into edge-connected components formed by triangles, and into oriented edge-connected sub-meshes. We describe the functionalities of *TopMesh* and the algorithms implementing them.

1 INTRODUCTION

A 3D object is most commonly described through a discretization of its boundary into a mesh consisting of triangles and of dangling edges, which do not bound any triangle. We call these meshes, known in algebraic topology as simplicial meshes, *triangle-segment meshes*. They are common in a variety of application domains, including computer graphics, solid modeling, finite element analysis, virtual reality, animation and scientific visualization. Triangle-segment meshes are specifically well suited for describing complex non-manifold objects. Informally, a *manifold* 3D object is an object in which the neighbourhood of every point on its boundary is topologically equivalent to a disk, or to a half disk. If the boundary of the object is triangulated, the manifold condition translates into the fact that the set of triangles incident at any vertex form a disk, or a half disk. Objects, that do not fulfil this property at one or more points, are called *non-manifold*, and if they also contain parts of different dimensionalities, are called *non-regular*.

While there exist tools to extract geometric and

topological information from manifold shapes, much less work exists on extracting such information from non-manifold ones. *TopMesh* is a tool for the extraction of topological information about a 3D object based on an analysis of its combinatorial representation. The basic idea, here, is translating topological properties in the continuum case into combinatorial properties of the discrete representation of the object as a triangle-segment mesh.

Triangle-segment meshes arise from the idealization of manifold triangular meshes obtained by the discretization of CAD models for finite element analysis.

Features of *TopMesh* are related to the extraction of non-manifold singularities, parts of the object boundary with different degrees of connectivity, and with different dimensions. Moreover, *TopMesh* allows computing a topological signature for a 3D object, given by the so-called the Betti numbers. Betti numbers provide a characterization of the topology of the object independent of the discretization of its boundary, which is particularly useful in shape analysis and retrieval. Betti numbers are topological quantities corresponding to the

connectivity of the object and to number of through-holes or handles, and of hollow cavities in the object.

TopMesh is implemented based on a library for encoding and manipulating triangle-segment meshes, the Triangle-Segment (TS) Library, freely available in (AIM@SHAPE, 2007).

The remainder of this paper is organized as follows. In Section 2, we provide the mathematical background with definitions and intuitive descriptions. In Section 3, we discuss related work, while in Section 4 we briefly describe the TS data structure. Section 5 is devoted to the description of the main functionalities of *TopMesh*, and in Section 6 we focus on the extraction of the Betti numbers. In Section 7, we presents results obtained on specific non-manifold datasets. Finally, in Section 8 we draw some concluding remarks.

2 BACKGROUND NOTIONS

In this Section, we introduce fundamental definitions as basis for our work.

We call a *triangle-segment mesh* any two-dimensional mesh discretizing the boundary of a non-manifold and non-regular three-dimensional object. Thus, a triangle-segment mesh is a two-dimensional simplicial complex embedded in the three dimensional Euclidean space (Agoston, 2005).

The basic entities in a triangle-segment mesh are triangles, edges that do not bound any triangles, that we call *wire-edges*, and vertices. The collection of all the vertices and edges of a triangle-segment mesh Σ form the *1-skeleton of the mesh*.

The *star* of a vertex v is defined as the set of triangles and edges that are incident at v . The *link* of v is defined as the set of edges and vertices in the star of v which are not incident in v (Agoston, 2005). Figure 1(a) and Figure 1 (b) show, respectively, the *star* and the *link* of a vertex. In a similar way, the star of an edge e is the set of triangles that are incident at e . The link of e is the set of vertices of the triangles in the star of e which are not extreme vertices e . Figure 1 (c) and Figure 1 (d) show, respectively, the star and the link of an edge.

A triangle-segment is *connected* when its 1-skeleton is a connected graph. A triangle-segment is *edge-connected* when, for every pair of triangles t_1 and t_2 of Σ , there is a path in Σ composed of an alternating sequence of triangles and edges such that any edge in the path is shared by two triangles preceding and following it. A triangle-segment mesh without wire-edges is just a triangle mesh. If it

contains at least one edge that is bounding exactly one triangle, it is called a *triangle mesh with boundary*.

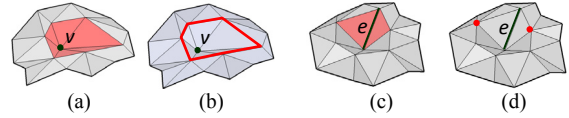


Figure 1: The star and the link of a vertex and an edge: (a) the star of vertex v ; (b) the link of vertex v ; (c) the star of edge e ; (d) the link of edge e .

A vertex v in a triangle-segment mesh is a *manifold vertex* if its link consists of one or two vertices, i.e., v belongs only to one or two wire-edges, or if the link of v consists of a closed or open chains of edges, i.e., v is shared by a fan of triangles forming a full disk (as in the example Figure 1(a)) or a half disk (in this latter case v is a *boundary vertex*). An edge is a *manifold edge* if its link consists of one or two vertices (as in the example Figure 1(c)).

A vertex, or an edge which does not satisfy the above properties is called a *non-manifold vertex* or *non-manifold edge*, respectively. Examples of non-manifold vertices and edges are shown in Figure 2, as their relative links.

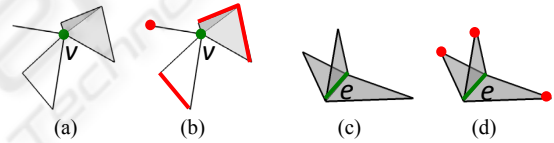


Figure 2: (a) The star of non-manifold vertex v consists of three components, one of which is a wire-edge and two of which consist of triangles; (b) The link of v for the example in (a); (c) The star of non-manifold edge e consists of three triangles; (d) The link of e for the example in (c) consists of three vertices.

The fundamental characterization of a three-dimensional object is given by its *Betti numbers* β_0 , β_1 and β_2 (Agoston, 2005). Specifically, β_0 is the number of connected components, β_1 is the number of 1-cycles, and β_2 is the number of 2-cycles. Intuitively, the 1-cycles define the independent tunnels, or handles, while the 2-cycles are parts of the object which enclose empty space (voids). A 2-cycle C in a triangle-segment mesh Σ can be viewed as an edge-connected component of Σ without boundary, such that the three-dimensional region enclosed by C is connected, that is, every two points in the region can be joined by a curve which does not intersect any simplex of Σ . Figure 3(a) shows an example of an object with one 1-cycle and one 2-cycle (the cube), while Figure 3(b) shows an example

of an object with two 2-cycles (the two cubes sharing a face). The Betti numbers are topological invariants and are independent of the way the object boundary is discretized.

On the other hand, the quantity $\beta_0 - \beta_1 + \beta_2$, which is called the Euler characteristic of the object, is related by Euler Poincaré's formula

$$n - e + f = \beta_0 - \beta_1 + \beta_2 \quad (1)$$

where n is the number of vertices, e the number of edges, and f the number of triangles in the triangle-segment mesh discretizing the object boundary.

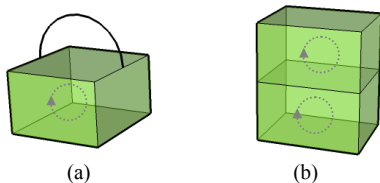


Figure 3: (a) An object formed by one 2-cycle and one 1-cycle; for this object: $\beta_0 = \beta_1 = \beta_2 = 1$; (b) an object with two 2-cycles, each of which is the interior of a parallelepiped; for this object: $\beta_0 = 1$, $\beta_1 = 0$ and $\beta_2 = 2$.

3 RELATED WORK

In this Section, we review some related work on topological segmentation of non-manifold shapes and on the computation of topological invariants.

In the literature, several techniques have been proposed for segmenting the boundary of a 3D manifold shape, see (Shamir, 2006) for a survey. Such techniques try to decompose an object into meaningful components, i.e., components which can be perceptually distinguished from the remaining part of the object. Some methods have been developed in CAD/CAM for extracting the so-called form features, like protrusions, depressions or through-holes, which produce a boundary-based decomposition of a 3D object guided by geometric, topological and semantic criteria, see (Shah, 1991) for a survey.

Much less work has been done on decomposition of non-manifold shapes. A common approach to represent a non-manifold shape consists of decomposing it into manifold components. Some techniques have been proposed in the literature for decomposing the boundary of regular non-manifold 3D shapes (called r -sets), i.e., for non-manifold shapes which do not contain dangling faces or edges, which are described by their boundary. In (Falcidieno and Ratto, 1992), the idea of cutting a

two-dimensional non-manifold shape into manifold pieces is exploited to develop compression algorithms. In (Delfinado and Edelsbrunner, 1995; Desaulnier and Stewart, 1992), a representation scheme based on the decomposition of an r -set into its manifold parts. In (Rossignac and Cardoze, 1999), a decomposition algorithm for non-manifold shapes is presented which minimizes the number of duplications introduced by the decomposition process. In (Pesco *et al.*, 2004) the authors propose a decomposition of a 2D cell complex based on a combinatorial stratification of the complex, inspired by Whitney stratification and a set of topological operators for manipulating it.

In (Delfinado and Edelsbrunner, 1995) an incremental algorithm is proposed for computing the ranks of the homology groups (Betti numbers) for simplicial 3-complexes embeddable in the three-dimensional Euclidean space R^3 .

The basic idea is to build a complex by adding one simplex at a time, and at each step the Betti numbers are updated to reflect the changes in the homology groups.

The authors discuss implementations of the algorithm that run in time $O(n\alpha(n))$ and $O(n)$, where n is the number of simplexes in the complex.

(Dey and Guha, 1998) present an approach to compute the generators of the homology groups for compacted triangulated 3-manifolds in R^3 . Then, they show that this approach can be applied to arbitrary simplicial complexes in R^3 , after thickening the complex to produce a 3-manifold homotopic to it. Finally, a classical algebraic approach to the computation of homology groups is discussed in (Guezic *et al.*, 1998).

4 THE TS LIBRARY

We recall that a triangle-segment mesh is encoded as a *Triangle-Segment* (TS) data structure. The TS data structure is the non-manifold extension of the indexed data structure with adjacencies, which is the most common representation for triangle meshes. It is compact and scalable and it supports efficient navigation algorithms (De Floriani *et al.*, 2004). The TS data structure encodes the triangles, wire-edges and vertices of the mesh. The wire-edges and the triangles are represented by encoding relations *wire-edge-vertex* and *triangle-vertex*, respectively.

- For each wire edge e , *wire-edge-vertex* relation associates the two extreme vertices with edge e ;
- For each triangle t , the *triangle-vertex* relation associates triangle t with its three vertices (see

Figure 4 (a).

The relation among a triangle t and its edge-adjacent triangles may involve an arbitrary number of triangles along each edge of t , since an edge can be non-manifold.

For compactness, the TS data structure stores, for each edge e of a triangle t , the two triangles that are immediately preceding and succeeding t around e , when the triangles incident at e are sorted in counter-clockwise order around e , as shown in Figure 4 (b)). We call such relation the *partial triangle-triangle-at-edge* relation. The counter-clockwise order of an edge e is defined by considering one of the two possible orientations of e and by applying the right-hand rule with the thumb pointing consistently with $v \rightarrow u$, if $e = (v, u)$ and the orientation $v \rightarrow u$ is chosen for e . If edge e is an interior manifold edge, the predecessor and the successor are identical and consist of the only other triangle t' which share e with t (see Figure 4 (c)). When there is no triangle adjacent to t along e , the predecessor and the successor of t are both t .

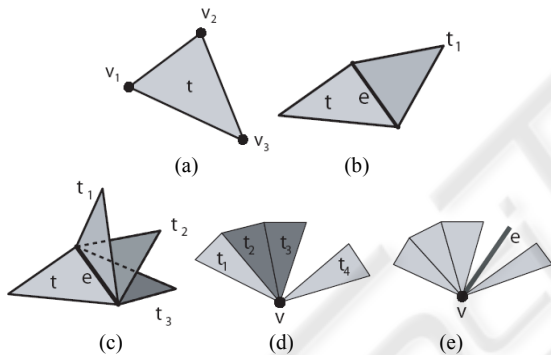


Figure 4: Topological information encoded in the TS data structure for a triangle t (a), for an edge e (b) (c) and for a vertex v (d) (e).

To simplify the task of navigating the mesh around a vertex, the TS data structure encodes for each vertex v (see Figure 4 (d-e))

- (i) the *vertex-triangle* relation, which associates with v one triangle for each edge-connected component in the star of v ;
- (ii) the *vertex-wire-edge* relation which associates with v all the wire edges incident at vertex v .

All the topological relations among the entities in the TS data structure (vertices, wire-edges and triangles) can be extracted in time linear in the number of entities involved in the relations (De Floriani *et al.*, 2004). The source code of the TS data structure library is freely available in an online tool repository (AIM@SHAPE, 2007).

5 BASIC FUNCTIONALITIES

We present here the basic functionalities of *TopMesh*, and describe the algorithms for extracting the topological information on which it is based. *TopMesh* extracts the following topological information from an object whose boundary is discretized as a triangle-segment mesh:

- *non-manifold singularities*: non-manifold vertices, non-manifold edges and wire-edges;
- components with various degrees of connectivity, namely connected components, *wire-webs*, which are maximal connected components formed by the wire-edges, and *edge-connected components*, which describe the parts of the object which do not contain non-manifold vertices;

In the following subsections we show how, relying on the TS data structure, *TopMesh* extracts the information listed above. In Section 6, we describe the computation of the Betti numbers, and specifically, we propose an algorithm for computing the number of 2-cycles.

5.1 Extracting Non-manifold Singularities

We consider a triangle-segment mesh encoded in a TS data structure. Wire-edges are explicitly encoded in the TS and thus their retrieval and counting is trivial.

A non-manifold vertex v is identified by counting the number of connected components in the link of v . This is performed by considering the *vertex-triangle* and *vertex-wire-edge* relations at v encoded in the TS data structure: v is manifold if only one of the two relations is not empty, and

- (i) if the *vertex-triangle* relation is not empty, and it consists only one triangle; or
- (ii) if the *vertex-wire-edge* relation is not empty, and it consists of either one or two wire-edges.

Otherwise vertex v is non-manifold.

A non-manifold edge e is detected by considering a triangle t incident at e and checking whether t has a predecessor and successor in the triangle-triangle-at-edge relation of t at e in the TS data structure, which are different. Otherwise edge e is manifold.

5.2 Extracting Connected Components and Wire-webs

Connected components of a triangle-segment mesh

Σ are identified by applying a connected component labeling algorithm to Σ . This is performed as a breadth-first traversal in the TS data structure. The traversal of each connected component starts at an arbitrary unvisited vertex v of Σ , and visits all triangles in the *vertex-triangle* relation encoded in the TS data structure, and all the wire-edges in the *vertex-wire-edge* relation at v . Then, all the vertices which are bounding such triangles and wire-edges are considered, and if they are not visited, they are inserted in a queue Q .

The traversal continues by extracting the first vertex in the queue and considering it as current vertex. A connected component is completely traversed when the queue is empty. By repeating this traversal process until no unvisited vertex is left, all the connected components are retrieved.

Wire-webs are connected components formed only of wire-edges. To detect and count such components, a traversal similar to the one described above is performed, but, at each vertex v , only the incident wire-edges are considered.

The edge-connected components are computed by considering the sub-mesh Σ' obtained from the original one Σ by eliminating all the wire-webs. The edge-connected components correspond to connected components of the dual graph representing Σ' . In the dual graph, the nodes correspond to the triangles of Σ' and the arcs to the edges shared by two or more triangles.

Edge-connected components are extracted from the TS data structure starting from an arbitrary triangle t of Σ' . For each edge e of t , all the triangles incident at e are extracted, marked as visited and inserted in a queue Q . Then, the first triangle in Q is extracted and the traversal is repeated from such triangle.

An edge-connected component is completely traversed when Q is empty. By repeating this traversal process until no unvisited triangle is left, all the edge-connected components are found.

It can be easily seen that all the above algorithms have a time complexity which is linear in the size of the mesh.

6 COMPUTING BETTI NUMBERS

In this Section, we show how to compute a topological signature of a 3D object based on its Betti numbers β_0 , β_1 and β_2 . Recall that β_0 is the

number of connected components, β_1 is the number of 1-cycles, and β_2 is the number of 2-cycles.

Given a 3D object represented as a triangle-segment mesh encoded with the TS data structure, β_0 can be computed as the total number of the connected components, β_2 needs to be computed by extracting oriented sub-meshes of the edge-connected components which enclose voids. Finally, β_1 is obtained from Euler-Poincare's formula by computing the number of vertices, edges and triangles in the mesh. Thus, the main step, here, is to compute β_2 .

In the following subsections, we first provide basic definitions and successively we present the algorithm for computing the number of 2-cycles.

6.1 Oriented and Folded Surfaces

The algorithm for computing the Betti number β_2 of a triangle-segment mesh Σ is based on the concepts of *triangle sides*, *oriented surfaces* and *folded surfaces*.

A triangle t has two triangle sides (with opposite normals) defined by the two possible orderings of its vertices. Each triangle side induces an orientation on each of its edges. In Figure 5 (a) an example is shown where the edge connecting vertices a and b has orientation $a \rightarrow b$ on one triangle side, and $b \rightarrow a$ on the opposite side. Two triangle sides are adjacent at their common edge e if one is reachable from the other by crossing e .

For each *edge-connected component* Γ in the mesh, we can extract connected collections of triangle sides for the triangles in Γ , that we call *oriented surfaces*. An *oriented surface* is a maximal edge-connected set of triangles sides, such that, for each pair of triangle sides s' , s'' in the set sharing an edge e , s' is the successor of s'' according to one orientation of e , and s'' is the successor of s' according to the opposite orientation of e . In other words, the two triangle sides that belong to two different triangles, which share a common edge, induce an opposite orientation on their common edge (see Figure 5 (b)).

To clarify the definition of oriented surface, let us consider the example shown in Figure 5 (c). Imagine an ant walking on the upper side of triangle t (that is T_1).

It reaches the triangle side U_1 by crossing edge (a, b) . It reaches the opposite side of t (T_2) by crossing edge (a, c) , because (a, c) is a boundary edge. An oriented surface is basically the surface formed by all the triangle sides that are reachable by a walking ant.

An oriented surface may enclose a void. An oriented surface S with boundary, such that for each triangle side s that belongs to S the other side s'' of the same triangle also belongs to S , cannot enclose any void.

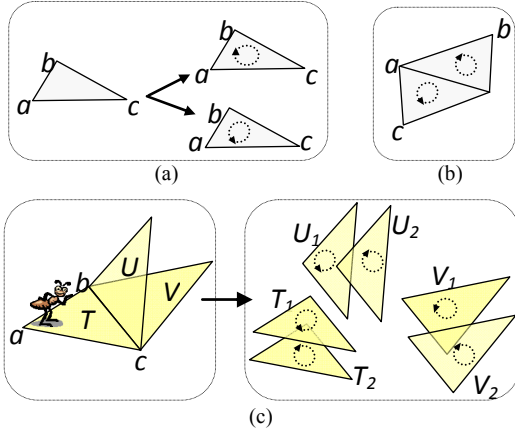


Figure 5: (a) Example of the two possible triangle sides for a triangle t (b) example of adjacency between two triangle sides. (c) example for an oriented surface. An oriented surface is basically the surface formed by all the triangle sides that are reachable (via adjacency) by a walking ant.

We call such oriented surface a *folded surface*. If an edge-connected component Γ consists of only one oriented surface, it must be a folded surface. Γ may consist of two surfaces, as it is always the case if it contains only manifold edges.

For instance, if Γ is a triangulated sphere, it consists of two oriented surfaces, each of which corresponding to an orientation of the surface of the sphere. If Γ consists of two triangulated cubes sharing a face, then there are three oriented surfaces associated with it, namely the two cubes with normals pointing towards the inside and the oriented surface consisting of the union of the two cubes with the normals pointing towards the external empty space (see Figure 6).

It can be easily seen that, if we consider an edge-connected component Γ of the original mesh, there exists exactly one oriented surface in the set of oriented surfaces associated with it, that we denote S_{out} , such that the normals to the triangle sides forming it point towards the outside space.

S_{out} defines a cycle of triangles which can be expressed as the linear combination of the other oriented surfaces associated with Γ . Thus, unlike the other oriented surfaces in Γ , S_{out} does not define a 2-cycle, since it contains the remaining oriented surfaces.

Note that, if Γ consists of one folded surface, this latter does not define a 2-cycle as well. Since there is exactly one oriented surface for each edge-connected component which does not define a 2-cycle, we have that the number of 2-cycles in the model is equal to the total number of oriented surface minus the number of 1-connected components.

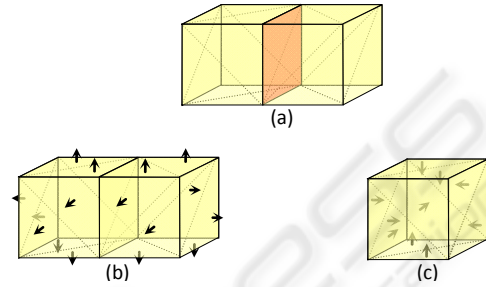


Figure 6: (a) Two triangulated cubes sharing a face; (b) the oriented surface with normals pointing towards the external space; (c) one of the two oriented surfaces with normals pointing towards the enclosed void.

6.2 Algorithm

The oriented surfaces in an edge-connected component Γ can be computed by defining a di-graph G_A on the collection of the triangle sides of Γ , that we call the oriented adjacency di-graph of Γ . In G_A , the nodes are the triangle sides, while there is a directed arc from a node s' to a node s'' if and only if the two sides s' and s'' share an edge e , and side s'' is the successor of s' at e . Note that graph G_A may contain parallel arcs oriented in the opposite direction since two sides of the same triangle can be the successors of each other at a boundary edge.

Figure 7 (a)-(c) show three examples of oriented adjacency di-graphs for (a) three triangles sharing a non-manifold edge, (b) two triangles sharing a manifold edge and (c) a triangle with a boundary edge.

Each strongly connected sub-graph of the oriented adjacency di-graph G_A defines an oriented surface. A strongly-connected component of graph G_A is any maximal subgraph H_A of G_A such that any node s'' in H_A can be reached from any other node s' of H_A through a directed path. If we consider all the triangle sides corresponding to the nodes in the strongly-connected component H_A , they form a maximal edge-connected set of triangle sides such that any pair of triangle sides s' and s'' are connected through a path on the complex formed by edge-adjacent triangles which are consistently oriented. Thus, they form an oriented surface.

We do not actually build the oriented adjacency di-graph, but we simulate it on the TS data structure. To this aim, we label each triangle t in the TS data structure with two bit flags.

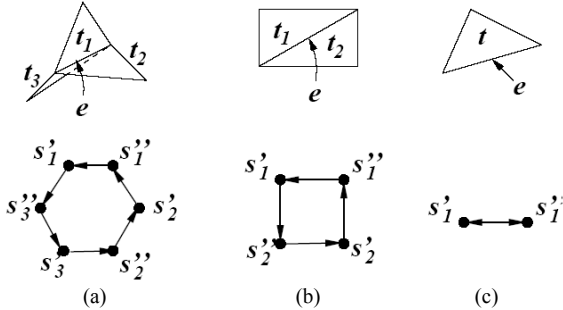


Figure 7: (a) Three triangles sharing a non-manifold edge e and the corresponding di-graph; (b) Two triangles sharing a manifold edge e and the di-graph at e ; (c) A triangle with a boundary edge e and the di-graph at e .

The first bit flag corresponds to the side of t defined by the order of the vertices of t as they are encoded in the *triangle-vertex* relation, the second one to the opposite side of t . A bit flag is equal to 0 if the corresponding side has not been visited, it is equal to 1 otherwise. The traversal of the directed arcs emanating from a node s' in the oriented adjacency di-graph corresponds to finding the successors of triangle side s' in the TS data structure along its three edges which have an orientation consistent with s' . Let us consider an edge e of s' and let s'' be the successor of s' in the oriented surface (and, thus, (s', s'') is an arc in G_A). We consider the triangle t corresponding to s' . Let the orientation of $e = (v, u)$ in the TS data structure be $v \rightarrow u$. We consider relation *triangle-triangle-at-edge* of t at edge e , which returns the pair (f_1, f_2) , where f_1 is the successor of t in counter-clockwise and f_2 is the successor of t in clock-wise order, according to the orientation of e .

Now, s'' will be a side of f_1 chosen in such a way that s'' induces an opposite orientation on edge e with respect to the one induced by s' . Note that, if e is a boundary edge, then $f_1=f_2=t$ and s'' is the other side of t with respect to s' .

Also, since the algorithm performs a visit on the di-graph G_A and the number of nodes in G_A is proportional to the number of triangles and edges in the input mesh, the algorithm complexity is linear in the size of the mesh.

7 DISCUSSION

TopMesh is a command line tool written in C++. It has been tested on several data sets on a dual-core 2.66GHz CPU, 1GB RAM WinXP platform.

In this Section, we show two examples of results of the application of *TopMesh* on non-manifold objects.

Figure 8(a) shows a table fan. It has a wire-web component (see Figure 8 (b)) and an edge-connected component (see Figure 8 (c)). Figure 8 (d) shows the table fan connectivity at non-manifold edges. The geometrical and topological data extracted by *TopMesh* for this model are summarized in Table 1. *TopMesh* also extracts the sub-meshes of the input meshes forming connected components, *wire-webs* and edge-connected components and also the oriented surfaces generated in the process of computing β_2 .

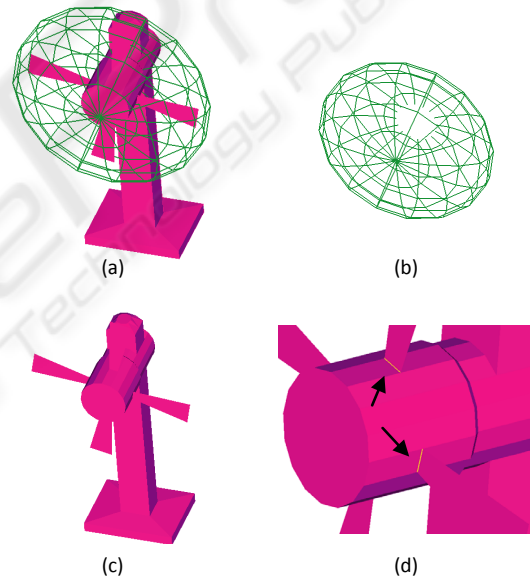


Figure 8: A non-manifold model representing a table fan (a). This model has a single wire-web in (b) and a single edge-connected component in (c). In (d) a zoom showing the non-manifold edges.

Figure 9 (a) shows a non-manifold model representing a chandelier. It has a wire-web component (see Figure 9 (b)) and 10 different edge-connected components (two of them are shown in Figure 9 (c)-(d)). Figure 9 (e) shows the chandelier connectivity at a non-manifold edge. The topological data extracted by *TopMesh* are summarized in Table 2.

Table 1: Topological information extracted by *TopMesh* from a non-manifold triangle-segment mesh representing a table fan.

Property	Value
Number of triangles	380
Number of Vertices	325
Number of edges	846
Number of wire-edges	272
Number of non-manifold vertices	145
Number of non-manifold edges	4
Number of wire-webs	1
Number of connected components (β_0)	1
Number of edge-connected components	2
Number of 1-cycles (β_1)	143
Number of 2-cycles (β_2)	1

Table 2: Topological information extracted by *TopMesh* from a non-manifold triangle-segment mesh representing a chandelier.

Property	Value
Number of triangles	18304
Number of Vertices	9242
Number of edges	27600
Number of wire-edges	136
Number of non-manifold vertices	80
Number of non-manifold edges	264
Number of wire-webs	1
Number of connected components (β_0)	1
Number of edge-connected components	10
Number of 1-cycles (β_1)	65
Number of 2-cycles (β_2)	10

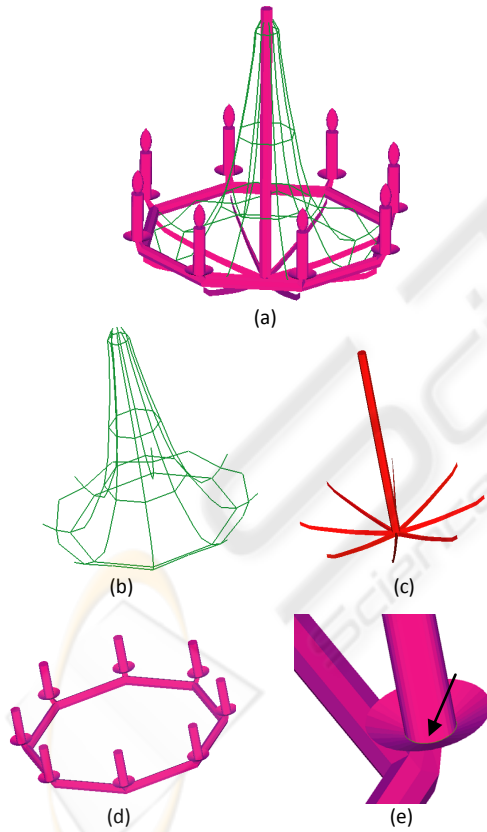


Figure 9: A non-manifold model representing a chandelier, which has a one wire-web (b) and 10 different edge-connected components - two of them in (c) and (d). In (e) chandelier connectivity at a non-manifold edge.

A web page presenting *TopMesh* and showing additional results, has been prepared and it is available at the following URL: <http://ggg.disi.unige.it/topmesh/>. On the web page the reader can eventually find additional material and images of the results.

8 CONCLUDING REMARKS

We addressed the problem of extracting topological characteristics from non-manifold 3D shapes containing parts of different dimensions, and discretized as simplicial complexes.

We presented *TopMesh* as a tool for the extraction of topological information by analysing a 3D object represented as a triangle-segment mesh encoded in the TS data structure. We showed how, by using the relations of the TS, we are able to extract topological information of the input mesh and we provided an algorithm for computing the topological 3D object signature via the Betti numbers.

Actually, *TopMesh* is being integrated as a core-module in a Semantic Web system (Papaleo *et al.*, 2007; De Floriani *et al.*, 2007), for inspecting 3D shapes and for structuring and annotating such shapes according to ontology-driven metadata. This system has been designed to support researchers in reasoning on digital shapes and in improving their knowledge about multimedia data available on the web.

As a further activity we want to extend the tool for performing a semantic-oriented decomposition of

a shape. This decomposition could be applied, for example, for classifying form features in simplicial shapes obtained as idealization of CAD models in the product analysis phase. Also, the decomposition can be the basis for a semantic-based annotation of complex 3D objects. We plan, also, to extend *TopMesh* in order to manage large non-manifold meshes using spatial indexing techniques.

ACKNOWLEDGEMENTS

This work has been partially supported by the MIUR-FIRB project SHALOM under contract number RBIN04HWR8, by the National Science Foundation under grant CCF-0541032, and by the MIUR-PRIN project on *Multi-resolution modeling of scalar fields and digital shapes*. The authors would like to thank May Huang for the support in the implementation

REFERENCES

- Agoston M. (2005) *Computer Graphics and Geometric Modelling: implementation and algorithms*. Springer.
- Campagna S., Kobbelt L., and Seidel H.P. (1998) "Directed edges a scalable representation for triangle meshes". *Journal of Graphics Tools*, 3(4):1–12.
- De Floriani L. and Hui A. (2007) "Shape representations based on simplicial and cell complexes". In *Eurographics 2007, State-of-the-Art Report*, pp.63–88.
- De Floriani L., Hui A., Papaleo L., Huang M., Hendler J. A. (2007) "A Semantic Web Environment for Digital Shapes Understanding". In *Lecture Notes in Computer Science, Semantic Multimedia, SAMT 2007*, vol.4816 pp. 226–239. Springer.
- De Floriani L., Magillo P., Puppo E. and Sobrero D. (2004) "A multi-resolution topological representation for non-manifold meshes". *Computer-Aided Design Journal*, 36(2):141–159, February.
- Delfinado C. A. and Edelsbrunner H. (1995) "An Incremental Algorithm For Betti Numbers Of Simplicial Complexes on the 3-Sphere". *Computer Aided Geometric Design*, 12(7):771--784.
- Desaulnier H. and Stewart N. (1992) "An Extension of Manifold Boundary Representation to R-Sets". *ACM Transactions on Graphics*, 11(1):40-60.
- Dey T. K., and Guha S. (1998) "Computing Homology Groups of Simplicial Complexes in R^3 ". *Journal of the ACM (JACM)* 45(2):266-287.
- Falcidieno B. and Ratto O. (1992) "Two-manifold cell decomposition of R-sets". In *Proceedings Computer Graphics Forum*, vol.11, pp.391-404.
- Gueziec A., Taubin G., Lazarus F., and Horn W. (1998) "Converting Sets of Polygons to Manifold Surfaces by Cutting and Stitching". In *Proceedings of the International SIGGRAPH'98*, pp.245-245 ACM Press.
- Munkres J. R. (1984) *Elements of Algebraic Topology*. Addison- Wesley, Redwood City.
- AIM@SHAPE NoE EC Network of excellence n.506766 (2007) www.aimatshape.net (last accessed Oct. 2009)
- Papaleo L., De Floriani L., and Hendler J., (2007) "Bridging Semantic Web and Digital Shapes", In *Proceedings of the International Eurographics Conference - Short Paper*, Prague, September.
- Pesco S., Tavares G. and Lopes H. (2004) "A Stratification Approach for Modeling Two-Dimensional Cell Complexes". *Computers and Graphics Journal*, (28):235-247.
- Rossignac J. and Cardoze D. (1999) "Matchmaker: Manifold B-Reps for Non-manifold R-sets". In *Proceedings 5th Symposium on Solid Modeling and Applications*, pp.31-41. ACM Press, June.
- Shah J. J. (1991) "Assessment of Features Technology". *Computer-Aided Design*, 23(5):331-343.
- Shamir A. (2006) "Segmentation and Shape Extraction of 3D Boundary Meshes". In *State-of-the-Art Report, Eurographics*, Vienna.